Proceedings of the Fifth European Conference on Underwater Acoustics, ECUA 2000
Edited by P. Chevret and M.E. Zakharia
Lyon, France, 2000

DO SNAPPING SHRIMP CHORUS IN TIME OR CLUSTER IN SPACE? TEMPORAL-SPATIAL STUDIES OF HIGH-FREQUENCY AMBIENT NOISE IN SINGAPORE WATERS

John R. Potter and Teong Beng Koay

Acoustic Research Laboratory, Tropical Marine Science Institute, NUS, 10 Kent Ridge Crescent, Singapore 119260. http://arl.nus.edu.sg email: johnp@arl.nus.edu.sg

Snapping shrimp dominate ambient noise over 2–300 kHz in warm shallow water. To investigate spatial & temporal behaviour, a stochastic tomographic inversion experiment & signal-processing algorithm have been designed. The experiment uses a set of directional hydrophones with parabolic acoustic mirrors steered in azimuth and elevation by onboard microprocessor systems with pitch and heading sensors. The hydrophones girdle an area of ~2000 m^2 of seabed in approximately 12m of water depth. Acoustic signals are acquired over 20-80 kHz. An initial deployment was conducted in March 2000. Raw time series clearly show snapping shrimp at all ranges. Horizontal anisotropy is of the order ±3 dB.

1. INTRODUCTION

It is now recognised that snapping shrimp dominate a vast bandwidth (from a few kHz to over 300 kHz) of ambient noise in warm shallow waters [1]. With increasing interest in higher frequency acoustics (above 2 kHz) in littoral regions an understanding of the temporal and spatial distribution of these animals' sounds is a pre-requisite for optimal system design and operation. Many researchers have recently become interested in investigating the 'snaps' that these animals make, either in the laboratory or by examining acoustic records of shallow-water ambient noise [2-6]. To date, there has been little work identifying how these animals are distributed spatially over scales of 10-100 m, or how their snapping behaviour is structured in time. Both spatial and temporal distributions need to be described statistically if these sources are either to be employed as Ambient Noise Imaging sources [7] or optimally-suppressed as the dominant noise in a conventional passive system. To achieve this statistical description for at least one typical site, a stochastic tomography experiment has been proposed [8]. The experimental design relies on two novel developments.

Firstly, the inversion algorithm to estimate the spatial source distribution from a series of overlapping, broadband acoustic 'footprints' from a set of directional acoustic receivers. This is a tomographic inversion, except that in this case the sources are random in space and time.

The 'stochastic tomography' algorithm and physical experimental layout were described in 1997 [8].

The second component is to develop the hardware capable of sampling the ambient noise field over a broad band, with high spatial resolution and with the ability to physically scan the environment. This is the aspect covered by this paper, in addition to presenting preliminary sample results from one of these directional, steerable hydrophones.

2. EXPERIMENTAL EQUIPMENT DESIGN

The experimental arrangement consists of a laptop- or desktop- PC data acquisition system on land and six self-contained remotely-controlled directional receivers at the wet end, each equipped with a Micro Controller Unit (MCU). The data acquisition system is an IoTech multi-channel A/D with total 1 MHz sampling rate, continuously streaming to a laptop through PCMCIA or desktop via PCI card. The PC directs the receivers to a desired look direction. The wet-end MCU's then initiate a procedure to turn and tilt the receiver until within tolerance of the requested direction, reporting back the actual pan and tilt values obtained. The control laptop then initiates the analogue sampling sequence for a predetermined period to provide a statistically stable sample.

2.1. The directional hydrophone

For the purpose of investigating snapping shrimp, the upper limit frequency of interest was taken to be 80 kHz, absorption taking too high a toll on the signal at ranges of interest ($O(10^2)$m) above this. At the other end of the bandwidth, too low a frequency would result in very poor directionality for a given aperture, and 20 kHz was selected to be the lower limit for this purpose. Wavelengths therefore varied between 19–75 mm. From geometric considerations, we sought an angular resolution of about 1 degree at the highest frequency, which meant that the two-dimensional spatial aperture would have to be of the order of about 1m to satisfy Rayleigh's condition. Since we must, in any case, be prepared to physically scan the system in azimuth and elevation, we can just as well use an aperture with a single fixed beam. The cheapest and most effective solution to this requirement is a parabolic reflecting dish.

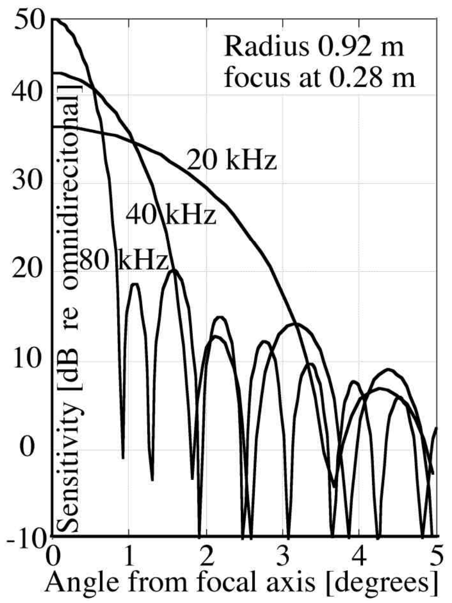

Fig. 1. Predicted beampatterns of a parabolic reflector at 20, 40 and 80 kHz in water.

The beampattern sensitivity of a parabolic reflector can be calculated theoretically following a Helmholtz-Kirchhoff approximation integrated over the reflecting surface. Deane has published such an analysis for a spheroidal reflector [9], and this approach was adapted to model a parabolic surface. Fig. 1 shows the results of this calculation for the parabolic reflector chosen for this experiment, with 0.92 m diameter and 0.28 m focal distance. Fig. 1 shows three curves, for 20, 40 and 80 kHz. The frequency-dependence of the main beamwidth is easily seen, roughly scaling with frequency. Using a broadband signal allows us to invert data with a wide range of ‘footprints’, according to the frequency, thus making the tomographic inversion more robust to error.

At each frequency, Fig.1 shows that even the most sensitive sidelobes are 30 dB or more below the main lobe. This is important to providing good signal to noise for the inversion, particularly when the main lobe is so small compared to the total solid angle available, 4 π. With a main lobe of only 1 degree or so (at the highest frequencies of interest), even sidelobes of average amplitude 40 dB below the main lobe can contribute (incoherently) to the signal in equal measure to the desired signal.

The directional hydrophone comprises not only the reflector, but also the hydrophone itself. The hydrophone must not only have the necessary bandwidth but must also be shielded to reject acoustic energy arriving from directions other than from the reflector. A custom-made ceramic spherical shell hydrophone was selected which was shielded by a foam collar to provide a receiving beamwidth matched to the apparent reflector size at the focal point.

The choices of reflector diameter and focal length were made to provide the best compromise between angular resolution, focal region position and hydrodynamic convenience. In currents of 1 m/s, even a 0.9 m parabolic dish can generate drag and lift forces O(10^2) kg. The reflecting surfaces were coated with 4 mm close-cell neoprene foam to provide a nearly perfect reflecting surface underwater. Each reflector was mounted on a stainless steel beam that also supported the electronics package, turned by a pan and tilt motor. Buoyancy balancing of the reflector and other items on the beam was achieved by attaching foam patches to the rear of the reflector to give a neutral pitch moment for the pan motor to overcome. A photograph of two of the reflecting parabolic dishes and hydrophones is shown in Fig.2.

Fig. 2. Two of the parabolic reflecting dishes and hydrophones.

Fig. 3. Hydrophone (at left), reflecting dish (white with black buoyancy patches on rear), frame (horizontal grey beam), pan and tilt motor (yellow) and electronics package (partially seen at right)

2.2. Mechanical support structure

A tripod provided support for the reflecting dish, hydrophone, wet-end processing electronics, battery box and pan and tilt motor. The tripod must elevate the reflector some 3m above the sea bed (to permit useful ‘look’ angles which intersect the bottom at not-too-shallow angles) and withstand some 100 kg force at that height. A custom stainless steel 316 (ss316) tripod was designed and manufactured locally. All joints were tongue and cheek, with sufficient clearance to remain operative even if infused with sand and fine grit, and pinned with ss316 gudgeons. The tripod legs terminated in broad footplates to prevent gradual sinking in sand and mud. All fasteners were inserted into through-holes, with a quick-securing latch to facilitate the divers' work. Visibility varied from 0.5-3.5 m 90% of the time. The tripod had extendable legs and a levelling table allowing both coarse and fine adjustment. A 100 kg (in air) concrete ballast weight was suspended by a 4:1 block and tackle from the base to improve stability and to take up slack in the system that could otherwise cause undesirable vibration and movement. No single component weighed over 90 kg in water and all items could be installed by divers using a 100 kg lift bag. Some 200 hours diving were logged in support of the experiment over 50 days. The general arrangement of the top of the tripod and receiver can be seen in Fig. 3.

2.3. Wet-end control & processing electronics

The wet-end control and processing electronics consists of an analogue data pre-processor (including pre-amplifiers, filters, line drivers etc) and a digital control module. Instructions are sent to the MCU by a multi-dropped, single master multiple slave RS485 serial link where each of the six slaves is given a unique address. The instructions specify a given desired azimuthal and elevation angle. The MCU reads a magneto-resistive flux sensor and inclinometer to assess the receiver's current orientation, then directs an underwater pan and tilt motor to turn and tilt until the desired look direction is achieved. The MCU then reports back the actual look direction obtained. The entire package is contained within a rigid PVC tube with piston and compressional "O" ring end seals, secured to the parabolic reflector support frame. A schematic of the components is given in Fig. 4.

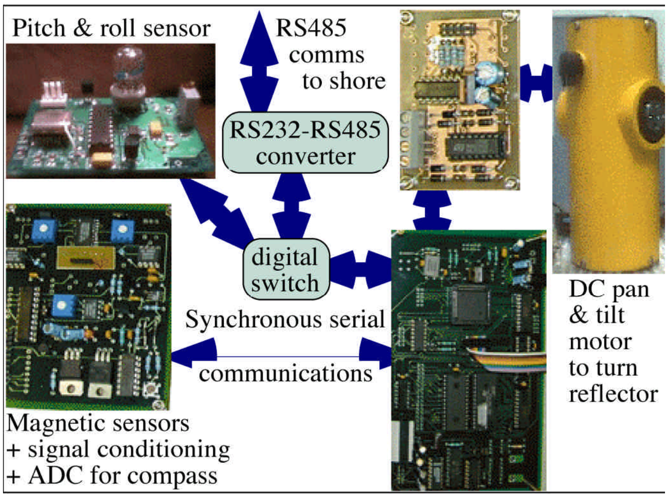

Fig. 4. Schematic and component photographs of the wet-end control components.

3. TIME SERIES EXAMPLE DATA

Although the entire six receivers and land-based systems were installed over a period of several weeks in March 2000, various teething troubles prevented sufficient data being taken to perform a stochastic tomographic inversion. After modifications are completed, we plan to re-deploy later this year. Meanwhile, preliminary data are available.

Fig. 5 shows a 5-second timeseries sample taken at zero tilt angle (looking horizontally). The characteristic sharp transients are due to snapping shrimp. A very few energetic snaps are seen (actually slightly truncated in Fig. 5 to save space) against a background of very many overlapping snaps of lesser amplitude. This is characteristic of a wide spatial distribution of snapping shrimp where those further away are more numerous, but each

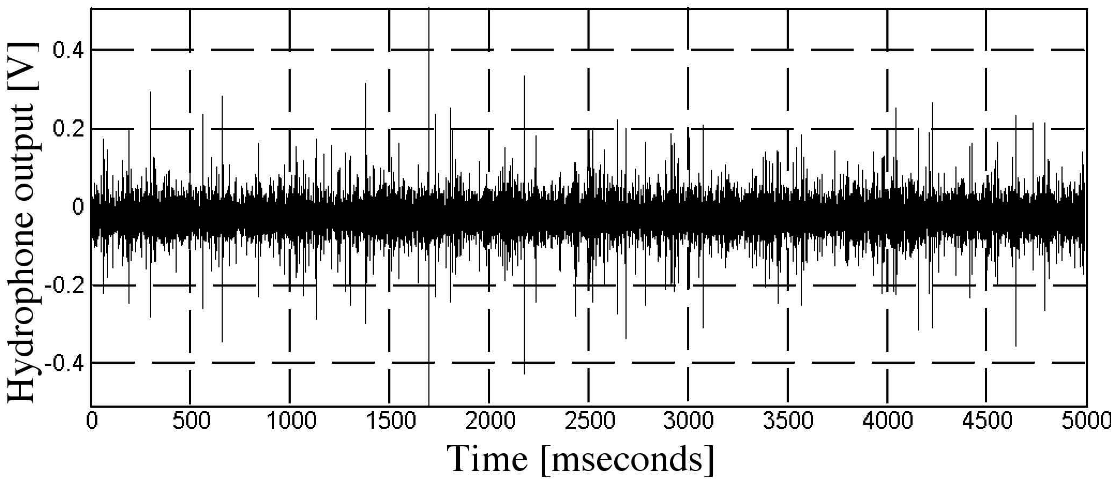

Fig. 5. Example 5s timeseries at zero tilt angle.

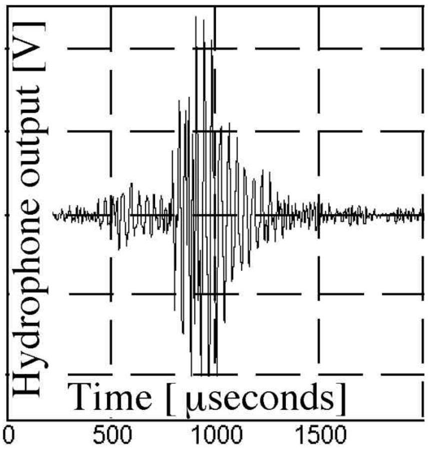

Fig. 6. Detail of a single 'snap'.

contributes less to the signal due to spherical spreading losses. Data taken tilted downwards, so as to receive from an elliptical footprint a few tens of metres long and a few metres wide, show lesser overlapping background activity and more local high-intensity activity as expected.

Examining just one of the high-intensity 'snaps', appearing as a single thin line in Fig. 5, reveals that it actually consists of a transient packet, including a relatively long ringing phase, and perhaps multiple reflected images (Fig. 6). There may also be a precursory oscillation to the main snap, a feature that has been suggested is associated with the claw closure rather than the supersonic ejection of the water spurt that is believed to be the primary cause of the sound.

4. HORIZONTAL ANISOTROPY EXAMPLE DATA

The site chosen for the experiment was a shallow (10-16 m) sand and mud basement area near Pulau Hantu, one of the Singapore southern islands. The site was expected to show some horizontal anisotropy in that deeper water lies to the south, and shallower water and corals lie to the west and east. These different habitats might be expected to provide varying degrees of suitability for snapping shrimp habitation. Fig. 7 shows a linear polar plot of the mean acoustic power received at one receiver as a function of azimuth, taken at night over several hours. Variations are ±3 dB about the mean and appear to line up approximately as anticipated with higher acoustic power being received from shallow areas and corals.

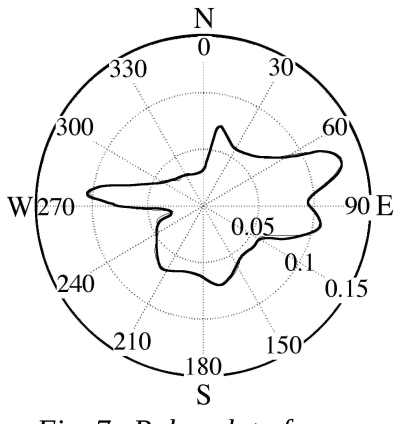

Fig. 7. Polar plot of mean acoustic power as a function of azimuthal direction.

5. DISCUSSION & CONCLUSIONS

The equipment development for the stochastic tomography experiment has provided six robust and intelligent directional hydrophone systems that are capable of recording ambient noise in shallow water over the frequency range 20-80 kHz. The systems were deployed in an area free from man-made structures. This is the first time that snapping shrimp noise directionality has been observed away from structures that are known to greatly influence snapping shrimp colonisation. Over the gently varying mud and sand at this site, ±3 dB horizontal isotropy is observed. The finding is supportive of the proposition that snapping shrimp provide good ambient noise illumination for ambient noise imaging, which requires both sufficient acoustic illumination and some isotropy in order to distinguish objects from background.

6. ACKNOWLEDGEMENTS

We are pleased to thank NUS who sponsor the project under grant RP3960679. Special gratitude to our biological friends and colleagues who helped us set up camp and provided much-needed infrastructure and also to the volunteer divers and boatmen who assisted in deployment and maintenance of equipment.

REFERENCES

[1] Hong, L., T.B. Koay, J.R. Potter and S.H. Ong. Estimating snapping shrimp noise in warm shallow water. *in* Oceanology International ‘99. 1999. Singapore: Spearhead Exhibitions.

[2] Au, W.W.L. and K. Banks. The acoustics of the snapping shrimp Synalpheus parneomeris in Kaneohe bay. Journal of the Acoustical Society of America, 1998. **103**(1): p. 41.

[3] Buckingham, M.J. and J.R. Potter. Observation, theory and simulation of anisotropy in oceanic ambient noise fields and its relevance to Acoustic Daylight imaging. *in* Sea Surface Sound '94. 1994. Lake Arrowhead, California, USA: World Scientific Press.

[4] Cato, D.H. and M.J. Bell. Ultrasonic ambient noise in Australian shallow waters at frequencies up to 200 kHz. DSTO internal report. 1991.

[5] Potter, J.R., T.W. Lim, and M.A. Chitre. Ambient noise environments in shallow tropical seas and the implications for acoustic sensing. in Oceanology International '97. 1997. Singapore: Spearhead Exhibitions Ltd.

[6] Readhead, M.L. Snapping shrimp noise near Gladstone, Queensland. Journal of the Acoustical Society of America, 1997. **101**(3): p. 1718.

[7] Potter, J.R. and M. Chitre. Ambient noise imaging in warm shallow seas; second-order moment and model-based imaging algorithms. Journal of the Acoustical Society of America, 1999. **106**(6): p. 3201.

[8] Potter, J.R., F.N. Wu, and L. Hong. A planned tomographic inversion experiment for snapping shrimp; temporal and spatial statistics of these primary noise producers,. in Shallow Water Acoustics Conference. 1997. Beijing: China Ocean Press.

[9] Deane, G.B. The beam forming properties of a concave spherical reflector with an on-axis receiver. Journal of the Acoustical Society of America, 1999. **106**(3): p. 1255.